EVALUATION OF DESIGN EQUATIONS ON THE UNIAXIAL COMPRESSIVE CAPACITY OF HOLLOW CIRCULAR HIGH-STRENGTH PRECAST CONCRETE-FILLED STEEL TUBULAR PILES

Clarissa JASINDA[1], Susumu KONO[2], Taku OBARA[3], Hiroshi HATTA[4], and David MUKAI[5]

SUMMARY

A hollow precast concrete-filled steel tube (CFST) pile is one of typical foundation piles commonly used in Japan for low- to mid-rise buildings. These piles are manufactured in factories with a centrifugal method using high-strength concrete (f_c'>80 MPa) and have the steel tube diameter-to-thickness ratio (D/t_s) from 50 to 100. Previous studies have investigated the uniaxial compressive behavior of hollow precast CFSTs and proposed expressions to calculate the axial compressive capacity of hollow precast CFSTs. However, these studies only cover hollow precast CFSTs with relatively small D/t_s (<50), and there is very limited data for hollow precast CFSTs with f_c'>80 MPa. This paper presents the experimental results on the compressive capacity of five hollow precast CFST piles. In addition, a database of uniaxial compression tests of 87 specimens is used to investigate the properness of existing design equations. The analysis results show a distinctive behavior of hollow CFST piles with f_c'>80 MPa where the capacity ratio ($N_{exp}/N_{(method)}$) distributions produce very steep regression lines. It suggests that the existing methods cannot accurately predict the compressive capacity of hollow precast CFST piles with high-strength concrete. These observations highlight the need to establish a new equation to evaluate the compressive capacity considering the influence of various parameters.

***Keywords**: CFST piles; precast pile; hollow cross-section; high-strength concrete; compressive capacity ratio.*

INTRODUCTION

Hollow precast concrete-filled steel tube (CFST) pile with circular section and high-strength concrete are common foundation members being used in Japan for low- or mid-rise buildings. These piles are used near the pile head where large shear force and deformation demands are expected during an earthquake. Hollow precast CFST piles are manufactured in the factory by centrifugal concrete casting technique using high-strength concrete ($f_c' > 80$ MPa). However, centrifugal casting was not used in this experiment. Instead, concrete was cast vertically, and a machine vibrator was used for consolidation. Compared to cast-in-place piles, hollow precast CFST piles are more economical, can speed up construction, and have superior quality control (Zhao et al., 2019). These advantages make hollow precast CFST piles more attractive to contractors and designers.

While hollow precast CFST piles are in use, by far, there are no dedicated standards or guidelines covering the design of these piles for severe earthquakes. The commonly used cast-in-place CFST design codes (AIJ, 2008; AISC 2016; EN 1994-1-1, 2004) do not have provisions to account for the hollow concrete core. These codes also limit the maximum compressive strength of concrete to about 80 MPa.

[1] *Graduate Student, Dept. of Architecture and Building Eng., Tokyo Institute of Technology, Japan, e-mail: jasinda.c.aa@m.titech.ac.jp*
[2] *Professor, Dept. of Architecture and Building Eng Tokyo Institute of Technology, Japan, e-mail: kono.s.ae@m.titech.ac.jp*
[3] *Building Research Institute, Japan, e-mail: obara.t.archi@gmail.com*
[4] *Concrete Pile and Pole Industrial Technology Association (COPITA), Japan, e-mail: h-hatta@m-sekisan.co.jp*
[5] *University of Wyoming, USA and Tokyo Institute of Technology, Japan, e-mail: DMukai@uwyo.edu*

A few studies have investigated the uniaxial compression behavior of hollow precast CFST piles. Miyaki et al. (1996[a]) carried out the uniaxial compression test of hollow precast CFSTs with concrete strength $f_c' = 51 \sim 94$ MPa. They observed that the axial compressive capacity of hollow precast CFSTs is higher than the sum of individual compressive capacities of concrete and steel tube. Based on the test results, they proposed an equation to calculate the compressive capacity of hollow precast CFSTs considering the concrete confinement contribution from the steel tube (Miyaki et al., 1996[b]). Okamoto et al. (1995) tested hollow precast CFST specimens with $f_c' = 101$ MPa. They found that the simple summation method of material strength contributions underestimated the compressive capacity when compared to the tested results. Zhao et al. (2019) proposed a formula to calculate the compressive capacity of hollow hollow precast CFST using test results of 70 specimens, of which 10 specimens had concrete strength of $f_c' > 80$ MPa.

Although these studies evaluated the compressive capacity of hollow precast CFSTs, the existing data is limited to f_c' less than 101 MPa. Accordingly, more experimental data—covering higher-strength concrete ($f_c' = 85, 105, 120$ MPa)—are required to understand the uniaxial compressive behavior of hollow precast CFST piles with high-strength concrete. Furthermore, the confinement contribution from the steel tube in hollow precast CFST is expected to be smaller, if any, for high-strength concrete compared to the normal-strength concrete. Therefore, there is a need to evaluate the existing equations to compute compressive capacity with the test results of hollow precast CFSTs.

This study presents uniaxial compression test results of five hollow precast CFST specimens to investigate the compressive peak and post-peak behavior. In addition, a database of hollow precast CFST piles consisting 12 specimens from the author's research group (Furukawa et al., 2020; 2021) along with 70 specimens data from past researches (Cai and Gu, 1987; Okamoto et al., 1995; Miyaki et al., 1996[a]; 1996[b]; Zhong, 2003; Kuranovas and Kvedaras, 2007; Wang et al., 2007) are collected. These data are then evaluated using existing methods, such as simple summation of material strength contribution, Sakino et al.'s (2004) equation, and Zhao et al.'s (2019) equation. Based on the comparisons, issues and limitations of the existing methods are discussed with recommendations for future investigations.

EXPERIMENTAL PROGRAMS

Specimen Details

Table 1 summarizes the technical details of the 12 hollow precast CFST pile specimens. The schematic cross-section details of these specimens are shown in Figure 1. The experimental variables shown in Table 1 are thickness of steel tube (t_s), thickness of concrete shell (t_c), presence of concrete infill – loaded or not loaded, and presence of soil cement. Specimens No. 1 and 2 are ¼ scale models of typical Ø800 hollow precast CFST piles commercially available in Japan. In the naming convention, "r" means that the hollow part of the specimen is filled with concrete infill, "u" means that there is a 1 cm thick layer of soil cement between the concrete shell and concrete infill, and "2" means the concrete infill is also axially loaded. The concrete shell was cast first, and soil cement and concrete infill were cast afterwards. Concrete infill was 120 MPa (high-strength) except for

Table 1 Details of hollow precast CFST pile specimens

No.	Specimen Name	D [mm]	t_s [mm]	t_c [mm]	Conc. Infill	Infill Loaded	Soil Cement	N_{exp} [kN]	N_0 [kN]	N_{exp}/N_0 [-]
1	SC25	190.8	2.3	25.8				1912	1930	0.99
2	SC25s	190.6	5.3	26.1				2594	2597	1.00
3	SC25ss	190.9	7.0	26.6				2654	2917	0.91
4	SC50	190.6	2.3	50.2				2864	2938	0.98
5	SC50s	190.7	5.3	51.3				3542	3571	0.99
6	SC25r	190.4	2.3	25.5	✓			1864	1911	0.98
7	SC25r2	190.5	2.3	25.5	✓	✓		3140	3536	0.89
8	SC25ru	190.5	2.3	25.4	✓		✓	1966	1907	1.03
9	SC25r2u	190.8	2.3	25.8	✓	✓	✓	2775	3105	0.89
10	SC25sr	190.7	5.3	26.3	✓			2438	2608	0.93
11	SC25ssr	191.2	7.0	26.5	✓			2558	2917	0.88
12	SC25r3	190.5	2.3	25.4	✓*			1756	1907	0.92

*Normal-strength (45 MPa) concrete infill. Other infill is high-strength (120 MPa).
N_{exp}: Experimetal compressive capacity; N_0: Computed compressive capacity, based on Eq. (1);
N_{exp}/N_0: Compressive capacity ratio, hereafter, capacity ratio.

SC25r3, whose concrete infill was normal-strength concrete of 45 MPa. The concrete infill was not loaded except for SC25r2 and SC25r2u. Height-to-diameter ratio of 1.5 was determined so that the specimens are categorized as short columns to avoid the effect of slenderness. Table 2 shows the measured mechanical properties of concrete, soil cement, and steel tubes used in the experiment.

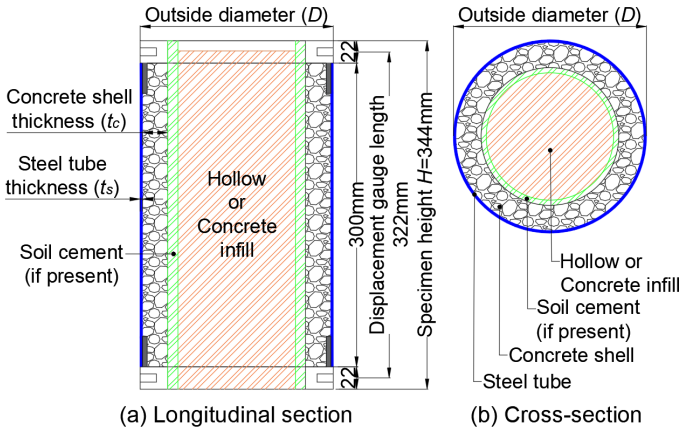

Figure 1 Cross-section details hollow precast CFST pile specimens

Table 2 Material Properties

(a) Concrete

	f_c' [MPa]	ε_c [μ]	E_c [GPa]	σ_t [MPa]
Concrete shell	120	2833	47.1	4.08
High-strength concrete infill	114	2843	46.8	4.58
Normal-strength concrete infill	45	2094	33.8	1.87

* The specimens were Ø100×H200 cylinders.
f_c' : concrete compressive strength; ε_c : concrete compressive strain at peak strength; E_c: Young's modulus of concrete; σ_t: concrete tensile strength.

(b) Steel tube

t_s [mm]	f_y [MPa]	ε_y [μ]	E_s [GPa]	f_t [MPa]
2.3	273	3400	195	413
5.3	351	3632	215	431
7.0	349	3621	215	426

f_y: steel yield strength; ε_y: steel yield strain; E_s: Young's modulus of steel; f_t: steel tensile strength.

Test Setup

Figure 2 shows the loading system. Uniaxial compression was applied to the specimens using 5 MN Universal Testing Machine (UTM). A universal joint was provided at the upper end of the 5 MN UTM. The average axial shortening was measured using two sets of displacement gauges with a gauge length of 322 mm. The two sets of displacement gauges were used to obtain the precise elongation at the steel tube surface. The loading was terminated when the post-peak load became nearly constant.

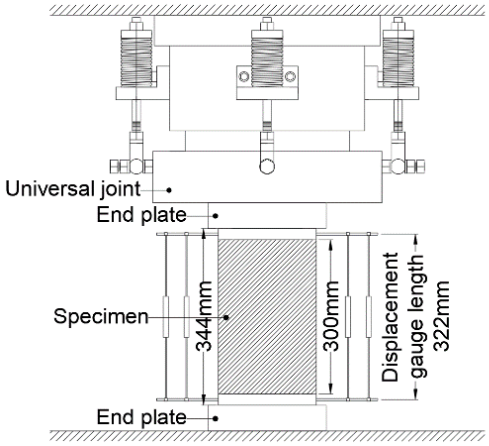

Figure 2 Schematic drawing of loading system

COMPRESSIVE LOAD (P) – AVERAGE STRAIN (δ) RELATIONSHIP

Figure 3 shows the $P-\delta$ relationship of the specimens. The average compressive strain δ was calculated from the average values of axial displacement gauges divided by the displacement gauge length (322 mm). The residual capacity ratios (in percentage) are added for each specimen. The capacity ratios (N_{exp}/N_0) are also added in the legend of each specimen, based on Table 1.

Figure 3(a) shows the influence of steel tube thickness (t_s) and concrete shell thickness (t_c) on the performance of specimens. The comparison between SC25, SC25s, and SC25ss indicates that the increase of steel tube thickness from 2.3 mm to 5.3 mm increased the compressive capacities of the specimens, but this effect was not observed for 7.0 mm steel tube due to premature failure of concrete. All these five specimens showed abrupt drops of axial load after the peak with similar degrading stiffness regardless of t_s or t_c. Strain ε_c was reached at the peak load, but the yield strain of steel was not fully reached yet for most of the specimens. Accordingly, the peak load would be expected to be less than the simple summation of capacities from concrete and steel (N_0 in Eq. (1)). However, the observed capacity (N_{exp}) nearly reached the simple summation, N_0, as indicated in the parentheses in the figure. The only exception was SC25ss which had $N_{exp}/N_0 = 0.91$. By observing the trend of N_{exp}/N_0 for SC25, SC25s, and SC25ss, it appears that steel tube thickness stopped influencing N_0 due to the premature failure of concrete. However, as the numbers in the parentheses indicate that methods of summation of capacities such as Eq. (1) may be applied to most cases, some adjustment may be necessary to account for the case of premature failure like SC25ss. It can also be inferred that the balance of t_s and t_c plays an important role for hollow CFSTs to reach the potential compressive capacities.

All five specimens in Figure 3(a) showed sudden post-peak drops with similar stiffness, regardless of t_s or t_c. The residual capacity ratio, however, increased with the increase of t_s as observed from the residual capacity ratio for SC25 (34%), SC25s (56%), and SC25ss (67%); SC50 (40%) and SC50s (50%). However, variation of parameter t_c shows inconsistent changes. With the increase of t_c, SC25 (34%) and SC50 (40%) showed a small increase in the residual capacity ratio. Yet, when comparing SC25s (56%) and SC50s (50%), the residual strength ratio did not increase.

Additionally, a test result of 2020 from the author's research group is included (TCR1) (Furukawa et al., 2021). This specimen is a cast-in-place CFST pile with filled concrete of $f_c' = 45$ MPa, specimen height $H = 300$ mm, outer diameter $D = 199.3$ mm, and $t_s = 2.3$ mm. When compared to five hollow precast CFST data, the compressive capacity degradation of cast-in-place CFST pile is more minor (with only 15% drop in residual strength percentage) and gradual. Hollow precast CFST piles, on the other hand, showed a sudden drop in capacity after the peak. This may cause a sudden loss of axial load-carrying capacity of pile foundations in buildings.

Figure 3(b) shows the effect of high-strength concrete infill presence. Concrete infill did not improve the peak strength of specimens because it was not loaded. However, the concrete infill greatly improved the post-peak performance and residual strength of specimens because the stability of the concrete shell greatly improved under a triaxial stress state. Comparing specimens SC25 (34%) and SC25r (58%); SC25s (56%) and SC25sr (80%); and SC25ss (67%) and SC25ssr (91%), residual strength ratio increases around 24% for specimens with high-strength concrete infill. During the loading process, the concrete shell was compressed until it deformed to the same height as the concrete infill, which resulted in the loading of the concrete infill in the later stage of loading. Thus, the capacity of SC25r, SC25sr, SC25ssr increased in the later loading stage.

Figure 3(c) shows the effect of concrete infill with different strengths and whether it was loaded or not loaded. SC25r2 shows that if the concrete infill is loaded, the peak strength of the specimen will be significantly improved, behaving similarly with cast-in-place CFST piles. The only difference is that the concrete infill and the concrete shell part are not monolithic, causing more prominent post-peak degradation compared with cast-in-place CFST piles (see the $P-\delta$ response of TCR1) in Figure 3(c). From the comparison of SC25r and SC25r3, the strength of concrete infill has no significant influence on the peak strength of specimens. Furthermore, concrete infill of SC25r3 was loaded accidentally after peak strength was reached. Hence, it cannot be concluded from this experiment if the strength of the concrete infill will have an impact on the residual capacity of the specimens.

Figure 3(d) shows the comparison of $\mathrm{P}-\delta$ Relationship for SC25r, SC25ru, SC25r2, and SC25r2u, which indicating soil cement's influence. The residual strength ratio of SC25r (58%) and SC25r2 (61%); and SC25ru (58.3%) and SC25r2u (58.9%) showed that when concrete infill is loaded, the residual capacity slightly increased. Another notable difference is that for the specimens with loaded concrete infill (SC25r2 and SC25r2u), the post-peak strength degradations decrease gradually instead of dropping suddenly. However, the presence of soil cement did not cause a meaningful increase of residual capacity in the case of not loaded concrete infill (comparing SC25r

to SC25ru), but it caused a slight decrease when concrete was loaded (comparing SC25r2 to SC25r2u).

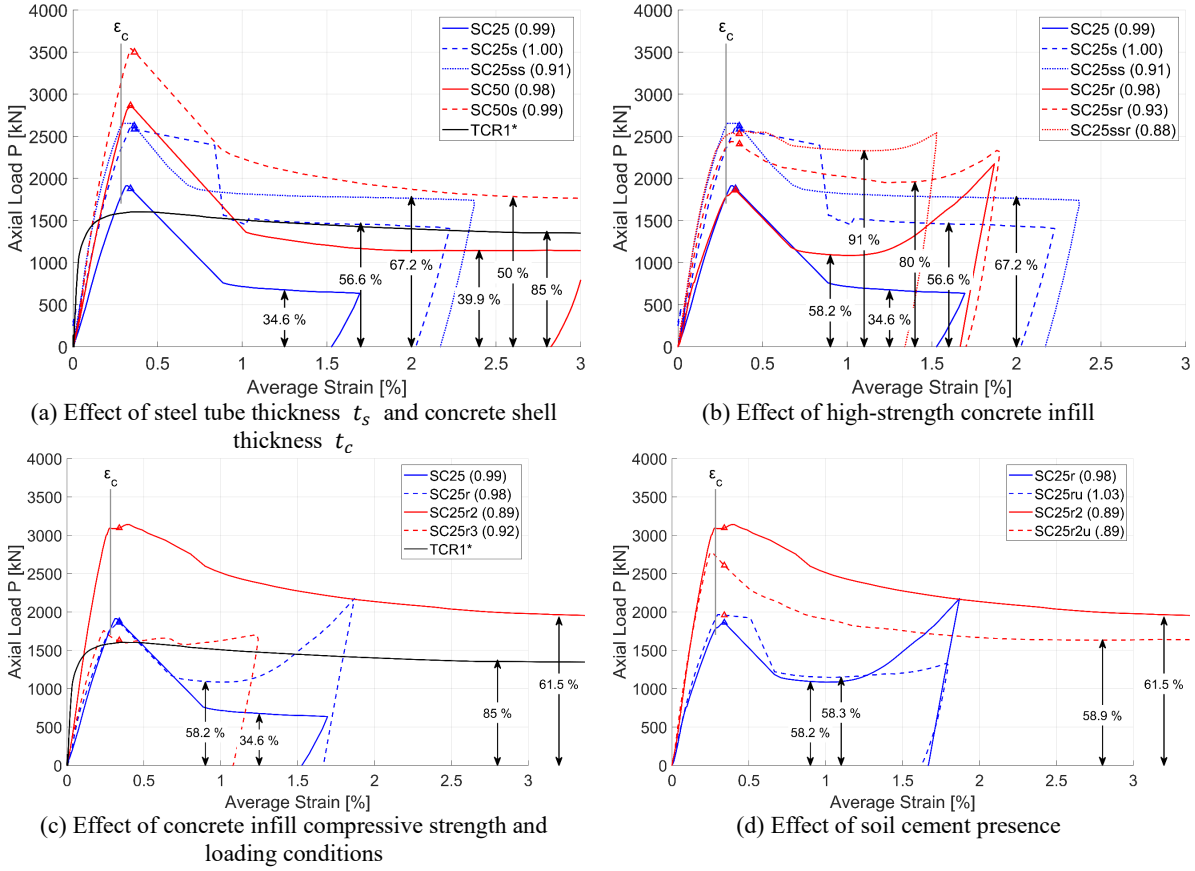

(a) Effect of steel tube thickness t_s and concrete shell thickness t_c

(b) Effect of high-strength concrete infill

(c) Effect of concrete infill compressive strength and loading conditions

(d) Effect of soil cement presence

* TCR1 is cast-in-place solid CFST pile specimen tested by author's group in the previous batch of compression test (Furukawa et al., 2021).
** Triangle symbols (△) marked in the figure are respective yield strains of steel tubes, ε_{y1}, ε_{y2}, and ε_{y3} in Table 2(b).

Figure 3 Compressive load (P) – average strain (δ) relationship

EVALUATION OF EXISTING DESIGN EQUATIONS

Axial Compressive Capacity Database and Evaluation of Hollow Precast CFST Specimens Under Uniaxial Compressive Loads (In Absence of Concrete Infill)

To further understand the behavior of hollow precast CFST piles, Zhao et al.'s database (2019) of 70 specimens, summarized in Table 3 (with hollowness ratio $\chi = 0.21 \sim 0.78$, $f_y = 172 \sim 391$ MPa, $f_c' = 23 \sim 101$ MPa, and $D/t_s = 23.8 \sim 148.0$), is evaluated along with 17 hollow precast CFST pile specimens from author's research group (listed as specimens No. 1~17 in Table 4). Table 4 includes five specimens from Table 1. To determine the basic behavior of the hollow composite section, only pure hollow specimens are included in the database. Specimens with concrete infill in the hollow part are excluded.

The compressive capacity of the collected specimens is evaluated using a simple equation expressed in Eq. (1), as well as methods proposed by Sakino et al. (2004) and Zhao et al. (2019) expressed in Eqs. (2) and (3), respectively.

$$N_0 = N_s + N_c + N_{ci} = f_y A_s + f_c' A_c + f_{ci}' A_{ci} \tag{1}$$

where N_0 is the nominal compressive capacity of hollow precast CFST pile; N_s, N_c, and N_{ci} are the capacities of steel, concrete shell, and concrete infill, respectively; f_y is the steel yield strength; f_c' and f_{ci}' are concrete shell and concrete infill compressive strengths; and A_s, A_c, and A_{ci} are the cross-sectional areas of steel, concrete shell, and concrete infill, respectively. N_{ci} is used for specimens where concrete infill was also loaded, i.e., No. 7 and 9 (whereas the concrete infill is not loaded, $N_{ci} = 0$).

Table 3 Summary of Zhao et al.'s hollow precast CFSTs database (2019)

No.	D (mm)	t_s (mm)	t_c (mm)	f'_c (MPa)	f_y (MPa)	N_{exp}/N_0	Ref.
1~12	165~166	3.5, 5.4	19~62	51~94	329, 351	1.13~1.23	(Miyaki et al., 1996[a]; 1996[b])
13~44	166, 200, 296	2.0~4.8	21~73	26~58	172~300	1.01~1.36	(Zhong, 2003)
45~46	166	4.4	52	23	249	1.41	(Cai and Gu, 1987)
47~65	300, 360	2.5~4.8	31~117	25~41	316~350	0.99~1.34	(Wang et al., 2007)
66~68	219~220	4.9, 5.0	27~29	30	361	0.98~1.00	(Kuranovas and Kvedaras, 2007)
69~70	200	5.95 8.42	64.1 60.7	102	391 371	1.06 1.14	(Okamoto et al., 1995)

Table 4 Circular hollow precast CFSTs database with high-strength concrete

No.	D (mm)	t_s (mm)	t_c (mm)	f'_c (MPa)	f_y (MPa)	N_{exp}/N_0	Ref.
1~6	200	2.3	25, 40, 60	100	290~325	0.83~1.19	Present Study (Furukawa et al., 2020; 2021)
7~12	199	2.3, 3.2	25, 40	125~130	244~385	0.82~0.96	
13~17	191	2.3, 5.3, 7.0	25, 50	120	273~351	0.91~1.00	
18~25	165~166	3.5, 5.4	31~62	82~94	329, 351	1.14~1.22	(Miyaki et al., 1996[a]; 1996[b])
26~27	200	5.95 8.42	64.1 60.7	102	391 371	1.06 1.14	(Okamoto et al., 1995)

Sakino et al. incorporated a coefficient of specimen size (α_c). This equation (Eq. (2)) is adopted by the AIJ guidelines for CFT members (AIJ, 2008).

$$N_{Sakino} = f_y A_s + \alpha_c f'_c A_c \tag{2}$$

where $\alpha_c = 1.67(D - 2t_s)^{-0.112}$.

Zhao et al. (2019) proposed an equation for circular hollow precast CFST based on a database of 70 specimens. A parameter called confinement coefficient (η_c) in Eq. (3) was included to amplify the strength of concrete. This coefficient includes the effect of the diameter-to-thickness ratio (D/t_s), hollowness ratio (χ), and material strength ratio (f_y/f'_c).

$$N_{Zhao} = f_y A_s + f'_c(1 + \eta_c)A_c \tag{3}$$

where $\eta_c = \frac{(1.8-2\chi^2)}{1-\chi^2}\left(\frac{t_s}{D}\right)^{(1-0.7\chi)}\left(\frac{f_y}{f'_c}\right)^{(1-\chi)}$; $\chi = \frac{d_c}{D}$; and $d_c =$ diameter of the hollow part.

Data from the combined databases are compared with calculated values in Figure 4 using Eqs. (1), (2), and (3). Results of capacity ratios ($N_{exp}/N_{(method)}$) are shown in the y-axis, where N_{exp} is the observed capacity from the tests. The x-axis is the concrete strength f'_c of hollow precast CFST piles. Regression lines are fitted from two groups of data: red regression line from Zhao et al.'s (2019) data of 70 specimens; and blue regression line from Table 4. The two regression lines share the same data of ten specimens (specimens No. 18~27 in Table 4). The coefficient of correlation (R) and the average value of the y-axis is shown for each regression line.

Figure 4(a) is shown as a benchmark. Comparing Figure 4(a) and (b), N_{exp}/N_{Sakino} is larger than N_{exp}/N_0 for all specimens due to the inclusion of coefficient α_c in Eq. (2). Figure 4(c) shows that Zhao et al.'s design method has a relatively accurate axial capacity prediction when evaluated on 70 specimens where the capacity ratio ranges between $0.85 \sim 1.16$ with an average of 1.02. However, when the method is evaluated with 17 specimens from the current research, the average capacity ratio is 0.81. This data for 17 specimens has higher concrete strength ($99 \sim 130$ MPa) than those of Zhao et al.'s dataset of 70 specimens. Zhao et al.'s proposed design equation (Eq. (3)) was calibrated based on a database of 70 hollow CFST columns, with 60 of them cast with normal-strength concrete ($f'_c < 80$ MPa). When evaluated on hollow precast CFST piles with high-strength concrete, the equation overestimated the compressive capacity for 24 out of 27 specimens.

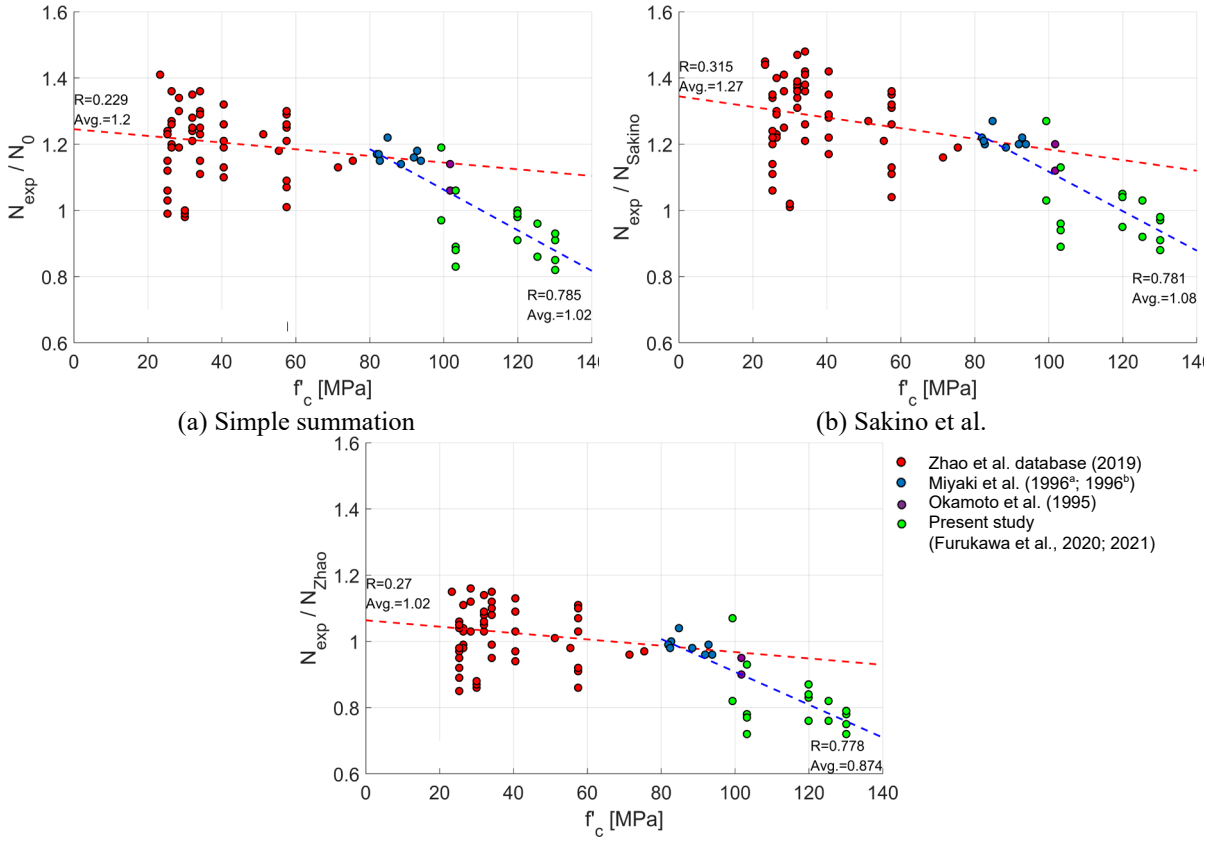

(a) Simple summation (b) Sakino et al.

(c) Zhao et al.

Figure 4 Distribution of compressive capacity ratio with concrete compressive strength f'_c evaluated with various design methods

Despite these differences, it is observed that there are similar trends in Figure 4(a), (b), and (c), where the blue regression lines have a larger slope than the red regression lines. There are also some outlier specimens, implying that there are other parameters (other than f'_c and aforementioned parameters in Eqs. (2) and (3)) that affect the compressive capacity of hollow precast CFST piles. From the above observations, there is an apparent need to establish a new design method for hollow CFST with high-strength concrete that considers the effect of various parameters, in addition to the parameters incorporated in Eqs. (2) and (3).

Compressive Capacity Evaluation of Specimens with Concrete Infill

In the previous research conducted by author's research group on the performance of hollow precast CFST piles under axial-flexural loads (Thusoo et al., 2020), it was found that infills in the hollow core can contribute to a significant improvement to the strength and ductility of the specimens. Hence, the uniaxial compressive performance is also deemed to be important to be studied, and the evaluation of the compressive capacity is presented in this subsection.

The specimens with concrete infill (No. 6-12) were cut in half to further observe the failure mode. Fluorescent solution was poured on the cut surface, and black light was used in order to observe the cracks clearly, as presented in Fig. 1.

When observing Figure 5(a) and (c), it is apparent that concrete infills in both specimens No. 6 and 8 do not show major crushing, while the concrete shells show crushing. The concrete infills of these two specimens were not loaded, and their N_0's were evaluated using Eq. (1)—where concrete infill capacity is not included in the nominal capacity. The failure mode aligns with the result from Table 1, where the N_{exp}/N_0 of specimens No. 6 and 8 are nearly 1.0. It showed that Eq. (1) can accurately predict the axial capacity of hollow precast CFST piles when the infill is not loaded.

Contrary to specimens No. 6 and 8, specimens with loaded infill (No. 7 and 9) show evident crushing of concrete infill (Figure 5(b) and (d)). Therefore, the inclusion of concrete infill capacity ($N_{ci} = f'_{ci}A_{ci}$), as expressed in Eq.

(1), is considered to be appropriate. However, based on Table 1, both specimens showed that N_{exp} is significantly below N_0, as indicated by N_{exp}/N_0 of 0.89, while their unloaded counterparts (specimens No. 6 and 8) have N_{exp}/N_0 of about 1.0. There is a need to include a reduction factor in $f'_{ci}A_{ci}$ to account for the inability of concrete infill to reach its full capacity. This inability is presumably caused by different failure timings. It is possible that the concrete shell failed before the concrete infill due to the instability caused by the hollowness of concrete shell.

Similar specimens were tested in previous experiments done by the author's research group for specimens SCR1-4 (Furukawa et al., 2021). These specimens had low concrete infill strength of $f'_{ci} = 21$ MPa, and concrete infill was loaded. However, results from that study showed that when N_0 was evaluated using Eq. (1) without including N_{ci}, N_{exp}/N_0 ranges between $0.99\sim1.05$. The N_{exp}/N_0's are close to 1.0, even when N_{ci} were not included in the total capacity. This indicates that since N_{ci} has to be included in the N_0 calculation (because concrete infill was loaded), there might be a need to incorporate reduction factor for either steel or concrete shell, in addition to the reduction factor for concrete infill.

Further investigations including wider range of concrete infill strength are needed to determine the reduction factors for concrete shell and concrete infill to better predict axial compressive capacity of hollow precast CFST piles.

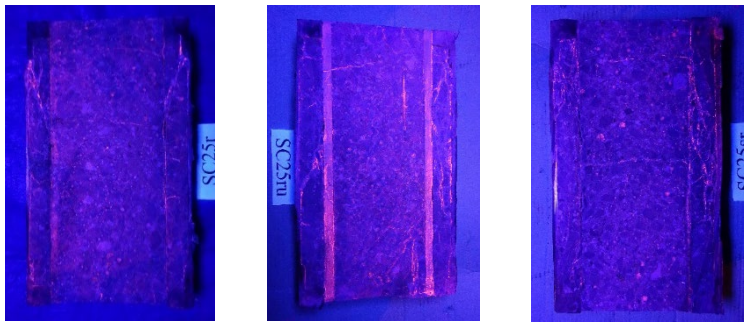

(a) SC25r (No. 6) (c) SC25ru (No. 8) (e) SC25sr (No. 10)

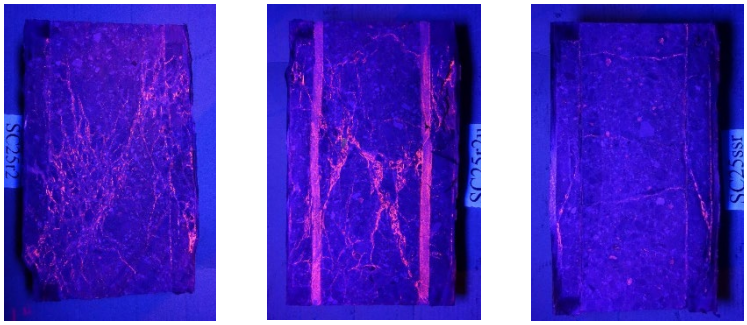

(b) SC25r2 (No. 7) (d) SC25r2u (No. 9) (f) SC25ssr (No. 11)

Figure 5 Failure modes for specimen with concrete infill

CONCLUSIONS

From the uniaxial compressive tests conducted on 12 hollow precast CFST pile specimens, and a database of 87 specimens including 70 from other literatures, the conclusions are as follows:

- The capacity of hollow precast CFST piles dropped abruptly with similar post-peak stiffness regardless of t_s or t_c after the peak strength was reached. However, the increase of t_s and t_c within a certain range can improve the performance of hollow precast CFST piles with high-strength concrete by increasing the compressive capacities and residual strength ratio.
- It is found that t_s and t_c should be designed in balance to avoid the premature failure of concrete and to obtain the full capacity of hollow precast CFST pile.
- Hollow CFST piles with high-strength concrete ($f'_c > 80$ MPa) showed a different tendency (more capacity degradation in terms of f'_c) compared to its normal-strength counterpart. The existing methods (guidelines and most recent study) cannot accurately predict the experimental results for high-strength concrete.
- The presence of concrete infill did not increase the compressive capacity but greatly improved the post-peak

performance in which the residual strength was increased, and the falling branch after the peak became a gradual drop instead of sudden drop. The strength of concrete infill did not have significant influence on the axial capacity. However, the axial load – displacement ($P - \delta$) performance was greatly improved if the concrete infill was loaded.

- Concrete infill capacity ($N_{ci} = f'_{ci}A_{ci}$) has to be included in the compressive capacity calculation when concrete infill is loaded. Capacity ratios (N_{exp}/N_0) and visual evidence suggest that a reduction factor is needed to account for concrete infill capacity reduction. In addition, it is found that the reduction factor for either steel tube or concrete shell might be necessary for hollow precast CFST piles.

ACKNOWLEDGEMENTS

The first author would like to express her sincere gratitude to MEXT, Japan for the funding of her Doctoral Studies at Tokyo Institute of Technology. The authors would like to thank COPITA for their valuable opinions. They also acknowledge the support from WRHI of Institute of Innovative Research and CRP of Laboratory for Materials and Structures at Tokyo Institute of Technology.

REFERENCES

American Institute of Steel Construction (2016). *Specification for Structural Steel Buildings (ANSI/AISC 316-16)*.

Architectural Institute of Japan (2008), *Recommendations for Design and Construction of Concrete Filled Steel Tubular Structures (2nd edition)*, (in Japanese).

Cai, S. H. and Gu, W. P. (1987), "Behaviour and load-carrying capacity of long concrete-filled steel tubular hollow columns," *Building Science*, Vol. 2, 11-20, (in Chinese).

EN 1994-1-1 (2004). *Eurocode 4: Design of composite steel and concrete structures-Part 1-1: General rules and rules for buildings*.

Furukawa, K., Jasinda, C., Ando, R., Obara, T., Kono, S., Mukai, D., and Watanabe, J. (2021), "Uniaxial compression test on precast and cast-in-situ CFST piles," *Summary of Technical Papers of Annual Meeting*, *AIJ*, Vol. IV, 603-606, (in Japanese).

Furukawa, K., Obara, T., Kono, S., Miyahara, K., Thusoo, S., and Mukai, D. (2020), "Uniaxial load test on scaled steel encased concrete pile specimens," *Summary of Technical Papers of Annual Meeting*, *AIJ*, Vol. IV, 575-576, (in Japanese).

Kuranovas, A. and Kvedaras, A. K. (2007), "Behaviour of hollow concrete-filled steel tubular composite elements," *Journal of Civil Engineering & Management*, Vol. 13, No. 2, 131-141.

Miyaki, S., Matsui, C., Tsuda, K., Hatato, T., and Imamura, T. (1996[a]), "Axial compression behavior of centrifugal concrete filled steel tubular columns using super high strength concrete," *Journal of Structural and Construction Engineering*, Vol. 61, No. 482, 121-130, (in Japanese).

Miyaki, S., Matsui, C., Tsuda, K., Hatato, T., and Imamura, T. (1996[b]), "Evaluation formula of compressive strength of centrifugal concrete filled steel circular tubular columns using super high strength concrete," *Journal of Structural and Construction Engineering*; Vol. 61, No. 482, 151-160, (in Japanese).

Okamoto, T., Maeno, T., Masuo, K., Nishizawa, H., and Kaneta, K. (1995), "Experimental study on the compressive strength of steel tube filled with high strength concrete using centrifugal compaction," *Journal of Structural and Construction Engineering*, Vol. 60, No. 469, 137-147, (in Japanese).

Sakino, K., Nakahara, H., Morino, S., and Nishiyama, I. (2004), "Behavior of centrally loaded concrete-filled steel-tube short columns," *Journal of Structural Engineering, ASCE*, Vol. 130, No. 2, 180-188.

Sakino, K., Yamaguchi, T., Nakahara, H., and Mukai, A. (2002), "Axial compressive load capacities of concrete filled circular steel tubular columns," *Summary of Technical Papers of Annual Meeting*, Vol. 48B, 231-232, (in Japanese).

Thusoo, S., Kono, S., Hamada, J., Asai, Y. (2020), “Performance of precast hollow steel-encased high-strength concrete piles,” *Engineering Structures*, Vol. 204, 109995.

Wang, H. W., Xu, G. L., and Zhong, S. T. (2007), “Study on influence of hollow ratio to bearing capacity of H-CFST,” *Engineering Mechanics*, Vol. 24, No. 10, 112-118, (in Chinese).

Zhao, Y. G., Yan, X. F., and Lin, S. (2019), “Compressive strength of axially loaded circular hollow centrifugal concrete-filled steel tubular short columns,” *Engineering Structures*, Vol. 201, 109828.

Zhong, S. T. (2003), “The concrete-filled steel tubular structures,” *Beijing: Tsinghua University Press*.